47th EPS Conference on Plasma Physics P2.1039

Progress in SCR-1: microwave heating scenarios calculations, magnetic field line tracing and new plasma diagnostics.

M.A. Rojas-Quesada[1], R. Solano-Piedra[1], A. Köhn[2], V.I. Vargas[1], L.A. Araya-Solano[1], A.A. Ramírez[1], M. Hernández-Cisneros[1], J.E. Pérez-Hidalgo[1], E. Meneses[3], D. Jiménez[3], Campos-Duarte, L[3]., F. Coto-Vílchez[1]

[1] *Plasma Laboratory for Fusion Energy and Applications, Instituto Tecnológico de Costa Rica, Cartago, P.O.Box 159-7050, Costa Rica.*

[2] *IGVP, University of Stuttgart, Germany.*

[3] *Advanced Computing Laboratory, Costa Rica National High Technology Center, CeNAT, San José, Costa Rica.*

INTRODUCTION

Stellarator of Costa Rica 1 (SCR-1) has been operational since June 29th, 2016 at the Plasma Laboratory for Fusion Energy and Applications at Instituto Tecnológico de Costa Rica. SCR-1 has a microwave heating system composed of two magnetrons of 2 kW and 3 kW and each generates microwaves at 2.45 GHz with a mean magnetic field = 41.99 [1]. Recently, MHD calculations and heating scenarios simulations have been made. Likewise, the diagnostics capacity is being enhanced with the addition of new diagnostics that add up to the ones already present in the device.

This work provides results related with the new calculations of the heating scenarios, magnetic field line tracing and the implementation of new diagnostics in the SCR-1 stellarator. Single O-X pass conversion with microwave heating scenarios at very low magnetic field (43.8 mT at the center) were performed by the IPF-FDMC full wave code [2]. These results were used to design a device capable of redirecting electromagnetic waves to plasma regions where O-X-B conversion takes place.

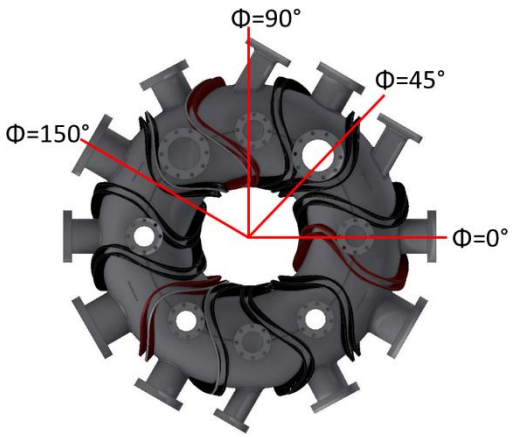

FIG. 1. Top view of the Stellarator of Costa Rica 1 (SCR-1) with some marked toroidal angles.

1.1. Single O-X pass conversion

The MHD calculations were made using the free-boundary mode in VMEC code. The results show that the outer magnetic flux surfaces bend more sharply than inner magnetic flux surfaces. This is indicated by a decrease of the rotational transform with the increase of the effective radius. The magnetic shear also decreases with the effective radius increase, which indicates the presence of a plasma region that is stable for the propagation of electron drift

47th EPS Conference on Plasma Physics P2.1039

waves. Additionally, there are significant plasma edge fluctuations that tend to increase with negative and low values for the negative and low magnetic well. The same behaviour for the fluctuations has been observed in the TJ-II, as reported from Castellano [3].

Previously, the vacuum magnetic flux surfaces were mapped [4] and compared with calculations made using Biot Savart Solver for Compute and Trace Magnetic Fields (BS-SOLCTRA), also the scientific visualization tool Paraview were used to simulate and visualize a 3D model magnetic field lines and flux surfaces [5].

Additionally, simulations of microwave heating scenarios were performed by the IPF-FDMC full wave-code [6]. These simulations calculate the conversion of the ordinary waves to extraordinary waves and the location of the region where the conversion was carried out. Moreover, the microwave heating scenarios for the toroidal position 330° are presented in Fig. 1. The microwave heating scenarios showed the O-X-B mode conversion around 12%-14%. Meanwhile, the electron Bernstein waves could be damped by ion-electron collisions. Therefore, it is necessary to know the ion density profile for the plasma of SCR-1 to calculate the ion-electron collision frequency.

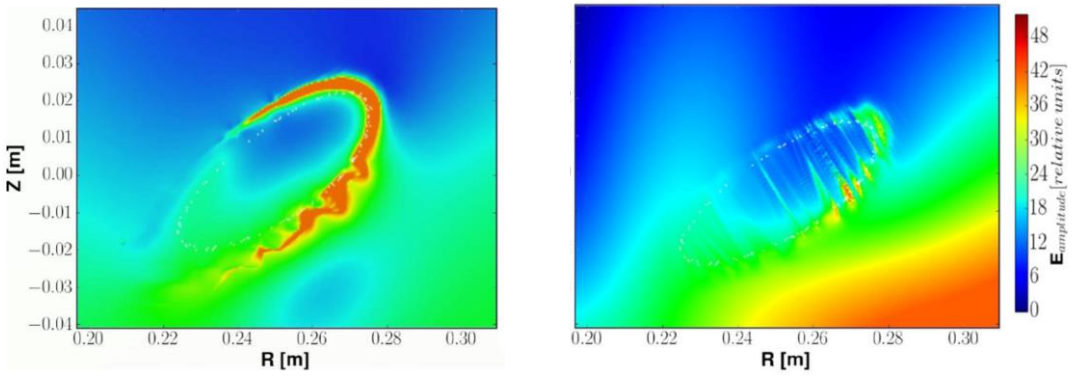

(a) (b)

FIG. 1. (a) Full-wave simulations at the 330° toroidal position for the injection angle of 58° after 20 periods of oscillation. (b) Full-wave simulations at the 330° toroidal position for the injection angle of 58° after 20 periods of oscillation with the magnitude of the magnetic field reduced to its fourth harmonic.

1.2. Bolometer design

The design of the case of the bolometer was based on the cylindrical geometry of the ports of SCR-1. The dimensions of the ports are 83.13 mm depth and 72.9 mm diameter. The case is made of three cylindrical stainless-steel pieces, as shown in Fig. 2. A pinhole of 0.8 mm diameter let the radiation hit the photodiode to measure the radiation energy emitted by the plasma. An electromechanical system was developed to auto-calibrate the position of the photodiode to get the maximum resolution to measure the radiation coming out from the stellarator. The bolometer will be installed in the toroidal position 150°.

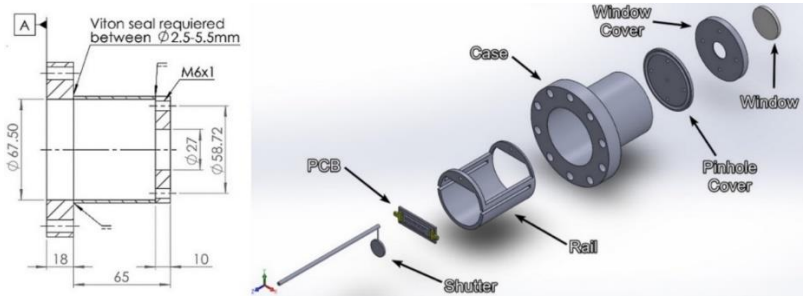

FIG. 2. Mechanical design of the bolometer.

47th EPS Conference on Plasma Physics P2.1039

The radiation energy will be measured through the integration of the viewing chords, as shown in the diagram in Fig. 3 It is also planned to introduce machine learning to enhance the data analysis from the diagnostic. The developed control system is based in two PSOCs. On the other hand, the acquisition electronics is made with an AXUV20ELGDS photodiode array of 20 elements and OPA4350 as transimpedance amplifiers. Both the mechanical and electronic systems are built (see Fig. 2) and the implementation of the diagnostic in the SCR-1 is expected to be done shortly.

The emissivity evaluation allows the estimation of the expected power in each of the photodiodes and therefore the current that could be measured in each channel of the Bolometer. The emissivity profiles and the expected signal in each diagnostic photosensor is a common calculation in fusion devices, however the results are distinct for any configuration of each experiment and the generated plasma. Thus, they are not directly comparable.

A computational code was written to estimate the emissivity due to the process of electronic transitions of the H y H_2, subject to the conditions of the plasma confined in the SCR-1. The emissivity profiles due to electronic transitions between the first levels of the singlet and triplet state of H_2, transitions between the first six levels of H, and the Bremsstrahlung process due to the interaction of electrons with H atoms were considered. For each case, conditions of maximum temperature and electron density expected during the discharge are assumed.

Using the emissivity, the brightness was also estimated. This is related to the expected signal in each photodiode of the bolometer and was calculated from the integral of the emissivity over a segment of the line of sight of the photodiode. The lines of sight of the photodiode were drawn considering the dimensions of the camera, the specific positions of the center of each photodiode and the distance between each and the pinhole. Therefore, this line corresponds to a straight line that begins from the center of each photodiode (20 in total), passes through the centre of the pinhole and ends at the last flow surface of the plasma. The lines of sight and the estimated brightness for each photodiode are shown in the Fig. 3.

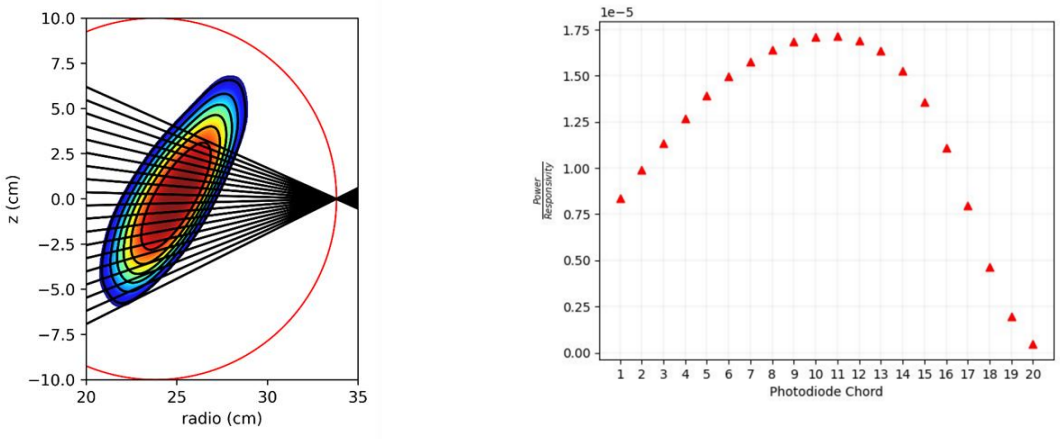

(a) (b)

FIG. 3. (a) Integration chords diagram and (b) estimated brightness at each photodiode for the bolometer design.

1.3. Magnetic diagnostics

The magnetic diagnostics are currently under different development phases. For each diagnostic, both control systems and mechanical designs were made. The magnetic diagnostics

47th EPS Conference on Plasma Physics P2.1039

follow the same principle of associating a voltage with an induced current from a magnetic signal. To calibrate the diagnostics a calibrating system was implemented using Helmholtz coils and Pasco CI-6520A magnetic sensors.

1.3.1. Diamagnetic loops

Two sets of diamagnetic loops are being designed. These loops will be located at toroidal positions 0° and 90°, both internally and externally from the vacuum vessel.

1.3.2. Rogowski coils

Rogowski coils are going to be located close to the bolometer port, both inside and outside the vessel. The Rogowski diagnostic is essentially a toroidal solenoid placed around the plasma volume aiming to register the magnetic flux passing through the solenoid interior. The coils are designed to measure signals coming from currents of 0.1 A and up to 1.0 A. This coil has been tested with ad hoc tests. These tests consist of placing a cable with variable current in the center of the coil and measuring the responsiveness of both the diagnostic and the integrating circuit.

1.3.3. Mirnov coils

The Mirnov coils sets will be located at 0°, 45°, and 90° on the toroidal axis angles. The poloidal distribution is not yet defined as it is not important for this stage. For this reason, the distribution will be defined following operational criteria during its implementation. The positions will be later optimized as MHD and magnetic topology studies go forward.

CONCLUSION

In summary, single O-X pass conversion with microwave heating scenarios at very low magnetic field (43.8 mT at the center) were performed by the IPF-FDMC full wave code. The microwave heating scenarios showed the O-X mode conversion around 12%-14%.
Using the field line tracer BS-SOLCTRA (Biot-Savart Solver for Compute and Trace Magnetic Fields) we were able to trace the magnetic field lines for the SCR-1 device. The vacuum magnetic flux surfaces were mapped and compared with the calculations, also the scientific visualization tool Paraview were used to simulate and visualize a 3D model magnetic field lines and flux surfaces. A flexible bolometer design and assembly is shown, as well as synthetic diagnostic estimations made for the device. Furthermore, new magnetic diagnostics were implemented as well, namely: a set of Mirnov coils, Rogowski coils and two diamagnetic loops which add up to the Langmuir probe.

REFERENCES

[1] VARGAS, V.I., et al, Implementation of Stellarator of Costa Rica 1 (SCR-1), in Proceedings of the 2015 IEEE 26th Symposium on Fusion Engineering (SOFE), May 31-June 4, 2015, Austin, Texas, USA
[2] KÖHN, A. et al, Plasma Physics and Controlled Fusion 55, 1 (2013).
[3] CASTELLANO, J. et al, Magnetic well and instability thresholds in the TJ-II stellarator. Physics of Plasmas 9. (2002)
[4] COTO-VÍLCHEZ, F et al. Vacuum magnetic flux surface measurements on the SCR-1 stellarator. In Proceedings of the 16th Latin American Workshop on Plasma Physics (LAWPP), pp. 43–46. IEEE. (2017)
[5] JIMÉNEZ, D. et. al, BS-SOLCTRA: Towards a parallel magnetic plasma confinement simulation framework for modular stellarator devices. In Communications in Computer and Information Science, Latin America High Performance Computing Conference (CARLA2019), pp. 33–48. Springer. (2020)
[6] VARGAS, V. I et al. Conversion of electrostatic Bernstein waves in the SCR-1 stellarator using a full wave code. In 27th IAEA Fusion Energy Conference (FEC 2018). IAEA. (2018)